Available online at www.sciencedirect.com
SCIENCE DIRECT®
Journal of Chromatography A, 1013 (2003) 111–122
JOURNAL OF CHROMATOGRAPHY A
www.elsevier.com/locate/chroma

# Effects of peak anomalies with the hydrophilic or hydrophobic properties of reservoirs during serial injection on a capillary electrophoresis microchip

Yun Seok Heo[a], Seok Chung[b], Keunchang Cho[b], Chanil Chung[b], Dong-Chul Han[a], Jun Keun Chang[b,c,*]

[a]*School of Mechanical and Aerospace Engineering, Seoul National University, San 56-1, Shinlim-dong, Kwanak-gu, Seoul 151-742, South Korea*
[b]*Digital Bio Technology, Co., Institute of Advanced Machinery and Design, San 56-1, Shinlim-dong, Kwanak-gu, Seoul 151-742, South Korea*
[c]*School of Electrical Engineering and Computer Science, Seoul National University, Kwanak, P.O. Box 34, Seoul 151-744, South Korea*

**Abstract**

Several anomalies, e.g., in peak shape, migration time, and baseline drift, all due to pressure-driven backflow, were previously reported to occur during serial injection on capillary electrophoresis (CE) chips. Since these anomalies were worse for polydimethylsiloxane (PDMS) microchips than for glass microchips, reproducible data on PDMS microchips were difficult to obtain. In this paper, we found that these problems were affected by the hydrophilic or hydrophobic properties of the reservoirs on the microchip and demonstrated that these anomalies were reduced by converting the hydrophobic properties of the reservoirs on the PDMS microchip into hydrophilic ones. Thus, compared with hydrophobic reservoirs, hydrophilic reservoirs were suitable for the formation of a stable plug. Several chip designs were suggested to reduce these pressure-driven backflows.


*Keywords:* Capillary electrophoresis; Peak shape; Polydimethylsiloxane

## 1. Introduction

Electrokinetic microfluidic systems, which have been studied by many groups, have been widely used in micro total analysis systems (μTASs), such as capillary electrophoresis (CE) microchips [1–7]. Up to now, the CE microchip has been used to analyze various substances, ranging from small drug molecules, amino acids, and oligonucleotides to large proteins and DNA fragments [8–11].

One of the advantages of the CE microchip is that it can be handled easily with various substances. Because the channel in a microchip is short (a few centimeters) and parallel compared with that of a conventional fused-silica capillary, various substances can be analyzed in a few seconds.

As we serially inject the samples in the microchannel, several unexpected problems arise. One

*Corresponding author. School of Electrical Engineering and Computer Science, Seoul National University, Kwanak, P.O. Box 34, Seoul 151-744, South Korea. Fax: +82-2-885-2267.
*E-mail addresses:* okhys@amed.snu.ac.kr (Y.S. Heo), jkchang@snu.ac.kr (J.K. Chang).

0021-9673/03/$ – see front matter 
doi:10.1016/S0021-9673(03)01359-1

particular fluid flow problem, that has been known to arise in both the capillary- and chip-based CE separations is the coexistence of undesired pressure-driven flow with electroosmotic flow (EOF). In a conventional CE system, to minimize any siphoning of the sample or buffer during injection, the liquid levels in the sample and destination vials should be kept even. Siphoning of the sample or buffer may cause unwanted variations of injection volumes, which, in turn, will give non-reproducible peak areas and heights and produce errors in the quantitative analysis [12]. Similarly, while performing CE separations on microfluidic chips, several anomalies such as peak shape, migration time, and baseline drift were reported by Crabtree et al. [13].

Although there are many factors that generate the pressure-driven fluid flow in CE experiments, it has been reported that the main factors are Laplace pressures generated at the meniscus of liquid–air interfaces, as well as hydrostatic flow due to the siphoning effect of the height difference between reservoirs (refer to Appendix A). Basically, if other parameters are constant during the experiments, the EOF pumping varies the level of the buffer in each reservoir. Hydrostatic flow will be proportional to the height difference between the buffer reservoirs [14]. Additionally, as the liquid volume in the reservoir changes, the meniscus stays anchored at the top edge of the reservoir, while the curved surface of the meniscus is seen to approach the bottom and sides of the reservoir. To minimize the surface free energy, flow will be driven toward the more empty reservoirs until the menisci are equal. Crabtree et al. demonstrated these facts and suggested that the Laplace pressure is more critical than hydrostatic flow for the separation anomalies on a glass chip. However, because, in real experiment processes, the combination of hydrostatic flow and Laplace pressure have an influence on the pressure-driven effect on the CE microchip, it is difficult to determine which factor is dominant.

In this paper, therefore, we aim to strengthen Crabtree et al.'s claims and suggest a new design condition for microchips. If the Laplace pressure, among the multi-factors that influence chip-based fluid flow, is more critical to hydrostatic flow, anomalies will depend on the hydrophilic or hydrophobic properties; the contact angle of the reservoirs will affect these phenomena. Thus, we assumed that hydrophilic or hydrophobic properties of the reservoirs on the microchip play key roles in the series of microfluidic manipulations and that material selections of reservoirs also have an important influence on the manipulations. By comparing the glass microchip with a PDMS microchip and the PDMS microchip with a glass tip vs. PDMS microchip with an octadecyltrichlorosilane (OTS)-coated glass tip, the validity of the assumptions were proved experimentally. In addition, we tried to reduce these anomalies produced by pressure effects. By designing the different channel length, we reduced these peak anomalies.

## 2. Experimental

### 2.1. Chip design

#### 2.1.1. Simple cross channel

The PDMS microchip consists of a cross-shaped intersection of a short and a long channel, 8 and 29 mm long, respectively, as shown in Fig. 1a. Channel size is 50 μm deep×50 μm wide. Each channel has 3-mm-diameter reservoirs at each end. The reservoirs are labeled sample reservoir (SR), sample waste (SW), buffer reservoir (BR), and buffer waste (BW).

#### 2.1.2. Length equivalent channel

To reduce the pressure-driven backflow, a longer channel-PDMS chip with channels of equal lengths of 24 mm was designed as shown in Fig. 1b. Besides the length and serpentine shape, other designs have the same conditions.

#### 2.1.3. Glass tip

For comparison with the PDMS chip without glass tips and with OTS-coated glass tips, a glass tube of 1 cm×3 mm I.D. was cut and bonded to each reservoir by epoxy.

### 2.2. Fabrication

The micro CE chip was made using soft lithography and replica molding [15]. A master was fabricated by spin-coating of negative photoresist

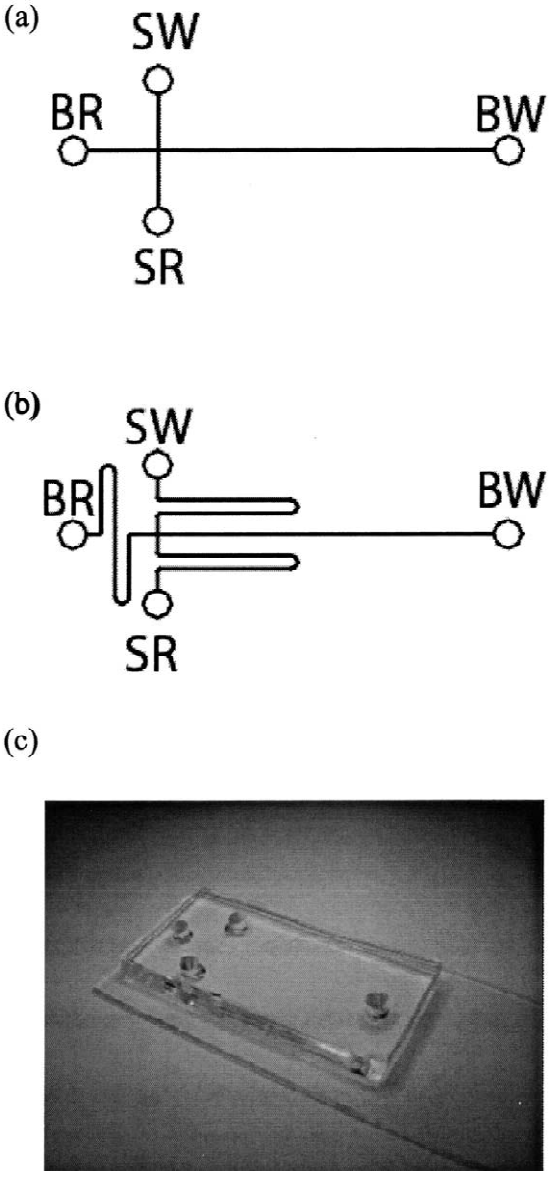


Fig. 1. Schematics of chips. (a) A cross-shaped PDMS microchip has a short and a long channel, 8 and 29 mm long, respectively. (b) A longer channel-PDMS chip with channels of equal lengths (24 mm). (c) Photograph of the PDMS microchip. Each channel has a 3-mm-diameter reservoir at each end.

(SU-8; MicroChem, Newton, MA, USA). A normal process includes spin coat, soft bake, expose, post expose bake (PEB) and develop. We molded the upper layer patterned by the micro channel on PDMS, cured and peeled them. Holes of 3 mm diameter were punched for the four reservoirs. An irreversible seal was formed between the PDMS layer and a slide glass to make a micro CE channel after surface treatment of $O_2$ plasma. Then the bonded chip was baked in an oven at 80 °C for 85 min to strengthen the bond.

### 2.3. Apparatus

The electrokinetic flow was controlled and detected by a laser-induced fluorescence detection system, DBCE$^{Tr}$ (Digital Bio Technology, Seoul, South Korea). The epiluminescence confocal detection module uses objective lens (40×, 0.55 NA) to focus the beam emitted from a frequency-doubled Nd:YAG diode-pumped solid-state laser (532 nm, 5 mW) onto a channel on the chip. Fluorescence is deflected and collected through a dichroic mirror toward the photomultiplier tube (PMT). The entire system was controlled by the LabVIEW program (National Instruments, Austin, TX, USA).

### 2.4. Reagents

The running buffer solution was prepared with 20 m*M* boric acid (Sigma, St. Louis, MO, USA) and adjusted up to pH 9.0. Fluorescein (Sigma) was dissolved in the same buffer at a concentration of 1 m*M* as a standard sample. The laser we used has a wavelength of 532 nm and generally uses rhodamine as a fluorophore. Fluorescein rather than rhodamine was selected because rhodamine is adsorbed by PDMS surfaces and plug generation is unstable according to the report of Slentz et al. [16]. A solution of 0.1 *M* NaOH was also prepared for cleaning microchannels. All the chemicals were reagent-grade and used as received. Each solution was filtered through a syringe filter of 0.2 μm (Minisart, Sartorius, Goettingen, Germany) before experiments were conducted.

### 2.5. Experimental procedure

#### 2.5.1. Pretreatment

Before the experiments, the microchannels for CE were thoroughly washed by applying a vacuum to one reservoir and filling up the microchannels with a 0.1 *M* HCl solution. Then, deionized (DI) water was

supplied in the other reservoir for 5 min each. The microchannels were also rinsed with a 0.1 *M* NaOH solution for 15 min to activate the PDMS surface. The DI water cleaning step was repeated, after which the microchannels were rinsed with 20 m*M* borate buffer and filled with the same solution. To stabilize the EOF, an electric field was applied to the microchannels for 5 min before sample loading.

#### *2.5.2. Octadecyltrichlorosilane coating*

First, glass tips or slide glass were cleaned by DI water–HCl (1:1) in the sonicator, and then a monolayer of OTS was deposited on the glass surface by immersing the cleaned glass into a 0.3% OTS toluene solution for 1 h.

### *2.6. Contact angle measurement*

The contact angle is the angle between the liquid and the solid surfaces when the liquid is thermodynamically in equilibrium with the solid [17]. Hydrophilicity and hydrophobicity can be defined with respect to the contact angle. A low contact angle means the surface has high wettability, high surface energy, and hydrophilicity; a high contact angle means the opposite and hydrophobicity. In general, glass is hydrophilic, PDMS is hydrophobic. Unmodified PDMS presents a hydrophobic surface with about a 100° contact angle, and the surface is prone to the adsorption of other hydrophobic species. Glass has about a 30° contact angle. OTS can convert the hydrophilic property into a hydrophobic one. Thus, by coating glass with OTS, we can make a glass surface similar to a PDMS surface. The measured contact angle of slide glass is about 31°, and after OTS treatment, the contact angle is 101°, which is similar to that of the PDMS surface, i.e., about 100°.

### *2.7. Injection method*

To introduce the sample, we used the pinched sample injection methods, which consist of two-step high-voltage controls. One step is injection and the other is a separation step. The schematic design and the two steps are shown in Fig. 2 (left). In the first step, the fluorescein sample in the sample reservoir started to move into the sample waste reservoir as

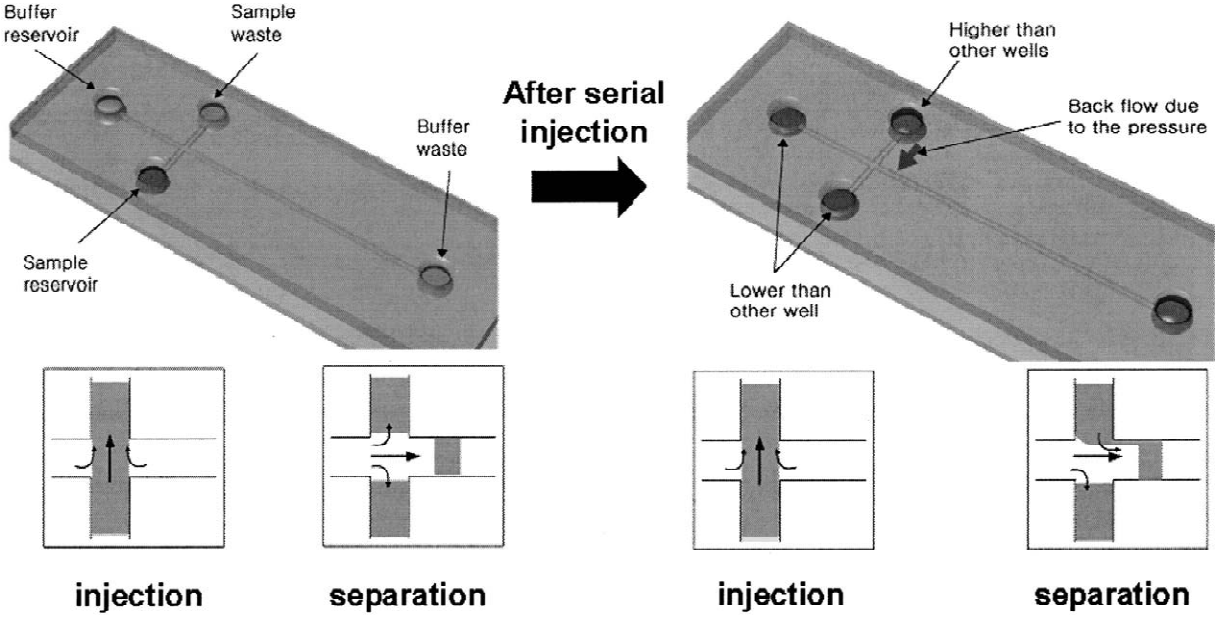


Fig. 2. Left is the normal pinched injection process. As the process continues, the sample reservoir is depleted and the sample waste reservoir (SW) is higher than before. After serial injection, back flow occurs due to the pressure effects, and the leakage from the sample waste reservoir produces problems such as peak shape, baseline drift, and migration time anomalies.

Table 1
Two-step high-voltage program used to form a plug of sample at the channel intersection and push it to the detection window for the simple channel micro CE chip

| Step | Reservoir potential (kV) | | | | Duration (s) |
|---|---|---|---|---|---|
| | Sample | Buffer | Sample waste | Buffer waste | |
| Injection | 1.5 | 1.1 | GND | 1.2 | 20 |
| Separation | 1.6 | 2.2 | 1.6 | GND | 30 |

the electric field was applied. Next, the electric field was switched to the second step, the separation mode, and the sample plug was introduced to the separation channel. The introduced sample plug was detected at the distance of 1.2 cm from the cross channel. The applied voltages are shown in Table 1.

## 3. Results and discussion

### 3.1. Anomalies with serial injection

As we previously studied, a series of injections of sample with a glass chip, purchased from Micralyne (Edmonton, Canada), were performed by repeating the voltage program in Table 1. The used volumes were 3 μl in each reservoir for the preliminary experiments. The same peak shape, baseline drift, and migration time anomalies, were obtained, as reported by Crabtree et al. As the experiments continued, the level of the SR gradually increased by EOF pumping. Thus, the leakage from SR occurred due to the Laplace pressure and hydrostatic flow, as shown in Fig. 2 (right). Thirteen serial injections in a glass chip were made, and the data depicting the separation anomalies are shown in Fig. 3a. Although no separation occurred with the single-component sample, it seems that a multicomponent sample is analyzed because of serial injection. When we applied the same conditions to the PDMS CE chip, though the buffer volumes were 4× larger than the glass chip, the results were severer than those of the glass chip, as shown in Fig. 3b. These peak shapes were inappropriate for the quantitative analysis of the sample concentrations and serial injection for the multi-port channels. As we discussed in the former section, the property of glass surface is hydrophilic and PDMS is hydrophobic. Although there are many factors, we considered that these discrepancies were mainly due to the use of different materials, especially hydrophilic or hydrophobic properties of reservoirs.

### 3.2. Comparison with each type of chip

To verify the effect of hydrophilic or hydrophobic properties of reservoirs, first, 3-mm-diameter glass tips were stood on the four reservoirs of the PDMS chip. By doing so, we are suggesting that, even though the internal channel is PDMS, the properties of outer interface parts of the reservoirs have an important influence on the manipulation in the microchannels. Each buffer volume with glass tips increases to 70 μl while the other factors such as chip designs remain the same. Compared with the PDMS chip without the glass tip, the anomalies are reduced and peak shape is stabilized, as shown in Fig. 4a.

We assume that these results are due to the larger buffer volume or hydrophilic or hydrophobic properties of the reservoirs. To decide which factors play the dominant role, we changed the glass tip's hydrophilicity to hydrophobicity by coating with OTS. When we conducted the experiments under the same conditions, the results were severer than those prior to the OTS treatment, as depicted in Fig. 4b. To understand how much the hydrophilic or hydrophobic properties affect these phenomena, only BR, among the four reservoirs, was coated with OTS while the others remained hydrophilic. According to the difference of capillary forces, the level of each reservoir was changed and buffer was dragged until the force difference was compensated with the height of levels, which are shown in the left side photograph of Fig. 4c. The contact angle of the glass tip was about 29°, and that of the OTS-coated glass tip

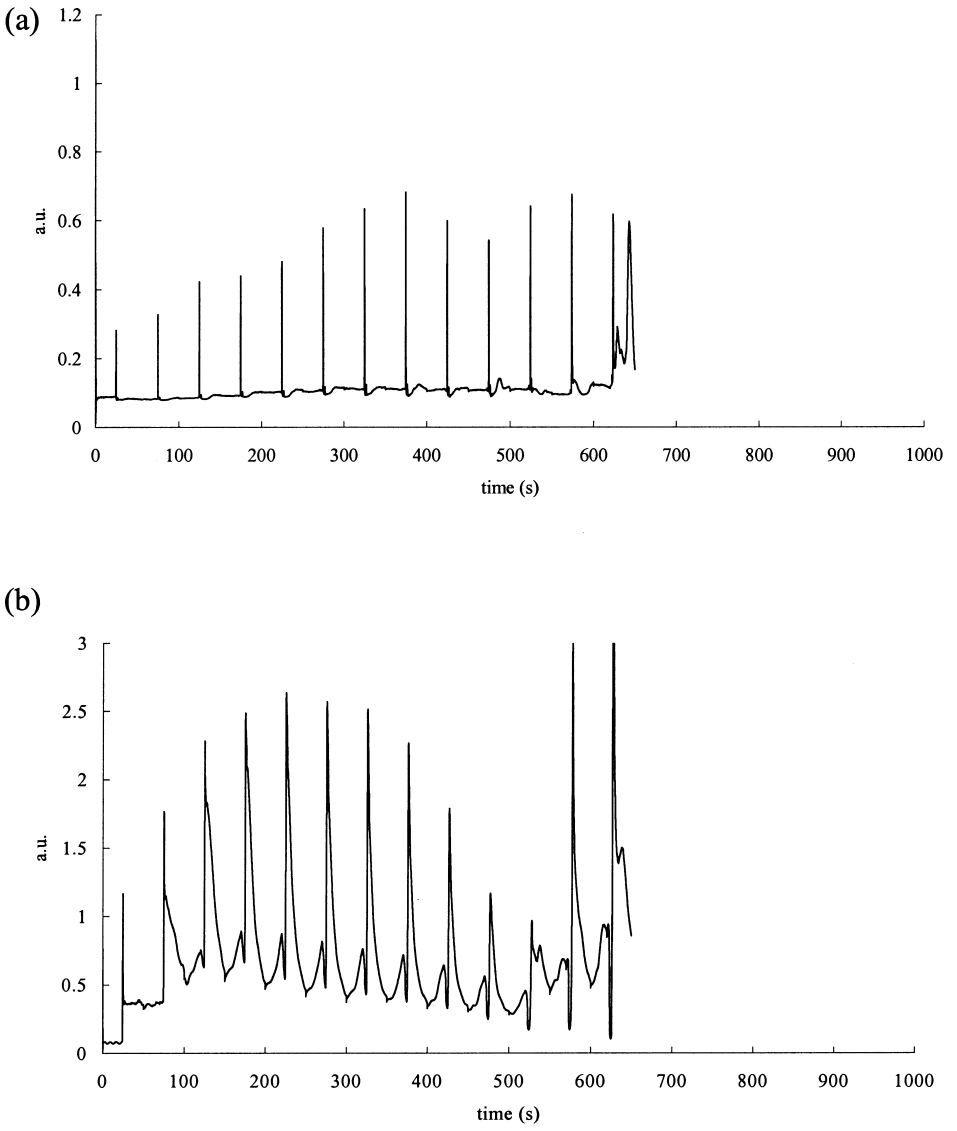


Fig. 3. The results of 13 serial injections on (a) a glass CE microchip and (b) a PDMS CE microchip, which show that (a) is more stable than (b).

was about 83°. All measured contact angles are summarized in Table 2. Because the level of the SW was already high when the electric field was applied, peak anomalies were at the most unstable state, as shown in Fig. 4c. Through additional experiments, we were able to confirm that hydrophilic or hydrophobic properties of the reservoirs significantly affected the serial injection.

### *3.3. EOF measurement*

To know the flow-rate in the microchannels, the EOF was measured by the procedure of Hung et al. [18]. Briefly, all of the microchannels and the reservoirs on the CE chip were, first, filled with 20 m*M* borate buffer, and then the buffer was replaced by 10 m*M* borate buffer. A high voltage was

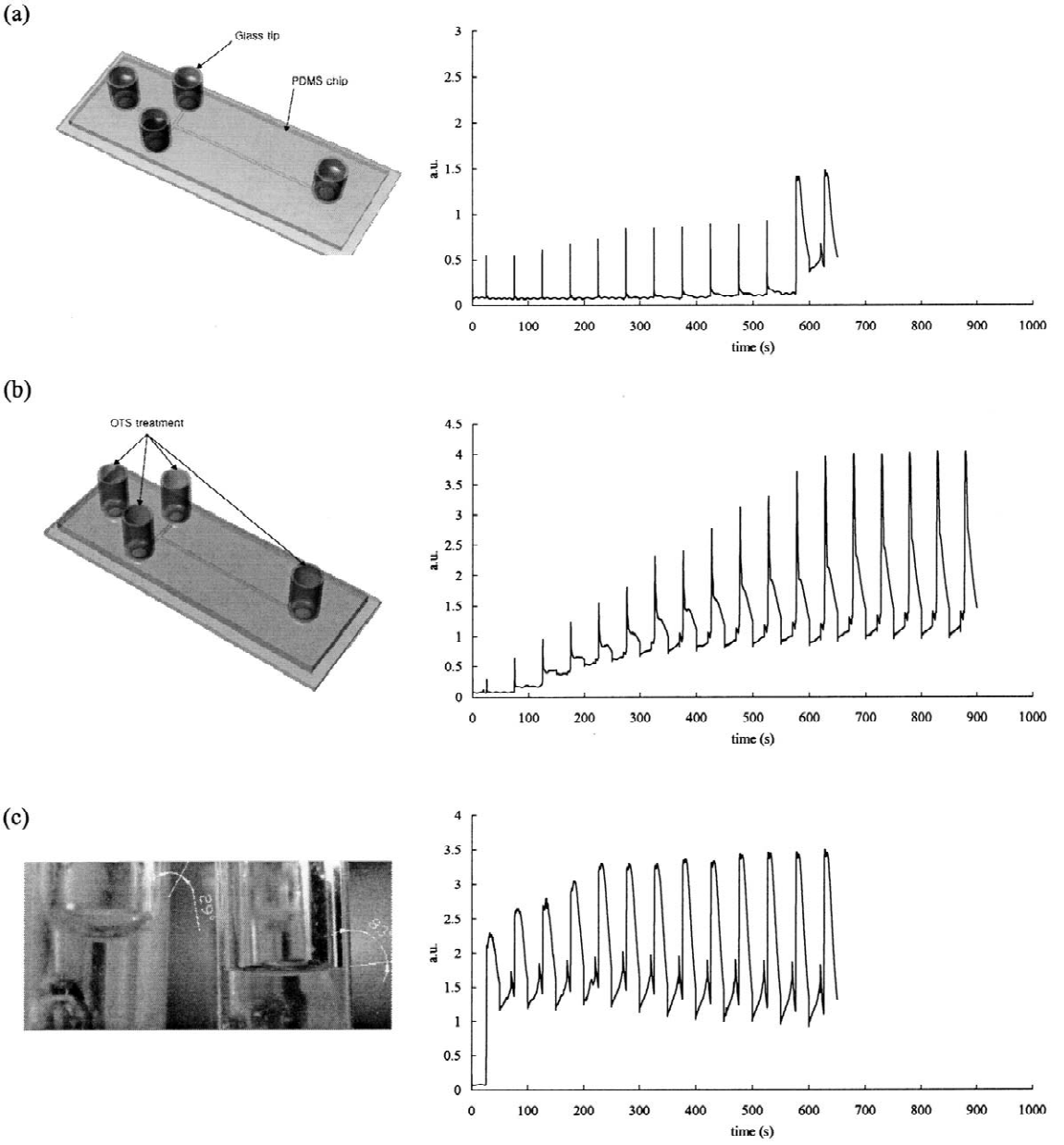


Fig. 4. The results of several serial injections on three types of CE microchips: (a) PDMS CE microchip with 3 mm diameter glass tips on PDMS reservoirs. Though serial injections are conducted on the PDMS CE microchip, the anomalies are weakened by standing of the glass tips. (b) Left diagram is the schematic design of the chip, and the experimental result shows that the OTS-treated surface, hydrophobic surface, is unstable compared with (a). (c) The result when only the buffer reservoir is treated with OTS. Due to the difference in Laplace pressure at each reservoir, buffer at BR flows into the SR and SW until the forces reach equilibrium. Because the buffer levels were different before the experiments began, the results are far severer than those in (a) and (b).

Table 2
All measured contact angles

| | Slide glass | Glass tip |
|---|---|---|
| Bare condition (contact angle, °) | 31 | 29 |
| OTS treatment (contact angle, °) | 101 | 83 |

Octadecyltrichlorosilane (OTS) treatment changes the hydrophilic surface to a hydrophobic one. The contact angle of slide glass is about 31°; after OTS treatment, the contact angle is 101°, which is similar to the one of the PDMS surface, about 100°.

applied across one of the microchannels while the others floated. As the 10 m*M* borate buffer replaced the 20 m*M* borate buffer, the time, *t*, was required for the current to stabilize, that is, for the 10 m*M* borate buffer to fill the entire channel. The velocity of the electroosmotic flow, $\upsilon_{eo}$, is given by:

$$\upsilon_{eo} = \varepsilon\zeta E/4\pi\eta \quad (1)$$

where $\varepsilon$ is the dielectric constant of the buffer, $\zeta$ is the zeta potential, $E$ is the applied electric field in V/cm, and $\eta$ is the viscosity of the buffer. The electroosmotic mobility, $\mu_{eo}$, of the buffer is given by $\mu_{eo} = \varepsilon\zeta/4\pi\eta$. The EOF velocity, $\upsilon_{eo}$, was determined by the relation $\upsilon_{eo} = L/t$ where $L$ is the channel length. The electroosmotic mobility, $\mu_{eo}$ may also be determined as follows:

$$\upsilon_{eo} = \mu_{eo}(V/L) \quad (2)$$

where $V$ is the applied voltage to the microchannel. Electroosmotic mobility is dependent solely on buffer characteristics, that is, dielectric constant, viscosity, pH, and concentration (which influence the zeta potential). Though the PDMS–glass hybrid microchip was used in this paper, distinguished distortions due to difference in zeta potential or surfaces were not found [19].

Here, we tested three types of chips: a PDMS chip, a PDMS chip with glass tips, and a PDMS chip with OTS-treated glass tips. When the data presented in Fig. 5a were compared with each other, the slope of the PDMS chip with glass tips was found to be steeper than those of the other chips and the PDMS chip appeared to be the most unstable. The change of slope in the PDMS chip may be due to the curved punching line because the menisci varied with the position of the curved reservoir, which was formed during the punching process. Generally, considering that the current across the channel is proportional to the flow-rate in the channel [20], we can assume that hydrophilic or hydrophobic properties of the reservoirs may affect this result. Fig. 5b and c clearly show our reasoning of the phenomenon that the hydrophilic surface is more stable than the hydrophobic one. Fig. 5b and c show the static and the dynamic status on the left and right, respectively. In Fig. 5b, when electric field was applied, the buffer started to flow and the menisci of each reservoir changed. Due to the anchor effect of the surface at the top edge of the reservoir and surface tension of water, the meniscus of the left reservoir was radically changed compared to that of the right reservoir. Though the direction of the EOF was from left to right, the flow by the Laplace pressure at each reservoir moved in reverse to the EOF, and thus the net flow was weakened and retarded. In the case of hydrophobic reservoirs, assuming the contact angle of about 90°, which is an appropriate assumption considering the result of Fig. 4c, the shape of the meniscus was near the horizon as shown in Fig. 5c. When the electric field was applied under this assumption, the shape of meniscus at the left reservoir was concave and the right one was convex because of the anchor effect and the surface tension of water. Therefore, the difference of Laplace pressure at each reservoir was aggravated and the net flow was weakened and retarded more than the hydrophilic one. This result is in accordance with sample leakages during the series of injections. Hence, we concluded that the hydrophilic property is more stable than than hydrophobic one. In our devices, the average electroosmotic mobility was determined to be about $4.3 \cdot 10^{-4}$ $cm^2/V\,s$, which is similar to the reported values [21].

### 3.4. How to reduce the peak anomalies

Additionally, we tried to reduce the anomalies in the serial injections. Separation techniques on chip generally require a unique chip design that can prevent anomalies under serial injection. In EOF, the fluid motion was driven principally by an applied electric potential rather than by a pressure force. Because these anomalies were mainly due to the pressure-driven flow, the channel resistance should have increased to minimize the pressure-driven flow.

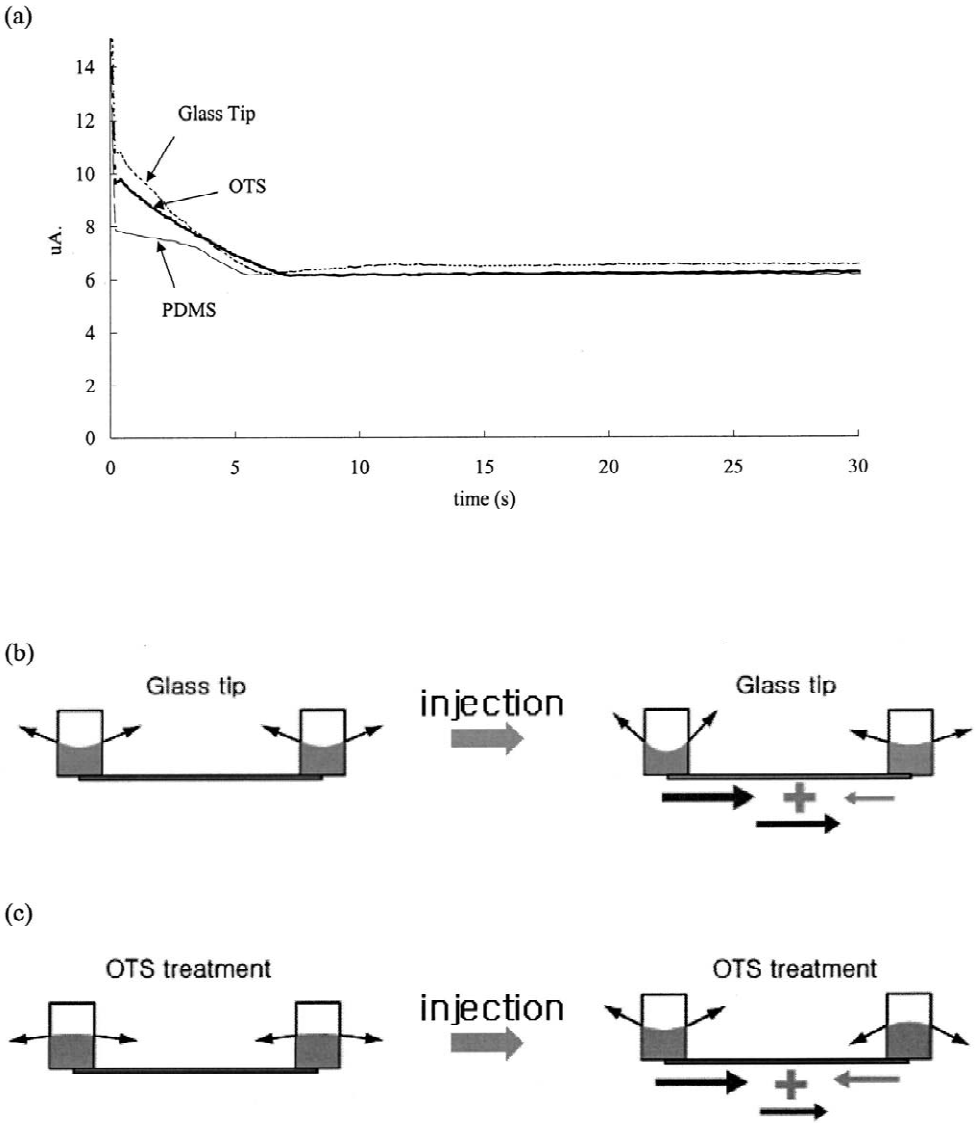


Fig. 5. (a) As the 20 m*M* borate buffer was replaced with the 10 m*M* borate buffer in the microchannel, the electric current dropped linearly with time according to the variations of channel resistance. Three types of the CE microchip were used. The slope of the CE microchip with a 3-mm-diameter glass tip is steeper than that of other types. (b) and (c) Show the reasons for the higher stability of the hydrophilic surface than that of the hydrophobic surface. Left is the static status and right is the dynamic status. (b) When electric field is applied at the microchip with the bare glass tip, the meniscus is changed at each reservoir and left reservoir is more radically changed than the right reservoir due to the surface tension of water. Laplace pressure at each reservoir acts in the counter direction and weakens the strength of the total Laplace pressure. (c) If the contact angle of the reservoir with OTS treatment is almost 90°, the difference of Laplace pressure at each reservoir, which is added during the dynamic condition, aggravates the pressure driven back flow due to the same directions.

A longer-channel PDMS chip with equal length channels of 24 mm was designed and induced two-step voltage conditions are shown in Fig. 6a. In general, as the channel becomes longer, pressure-driven back flows are reduced. Fig. 6b and c show that these anomalies are alleviated compared to those in Fig. 3b. Different buffer volumes, 13 μl for (b) and 10 μl for (c), were used. When (b) was compared

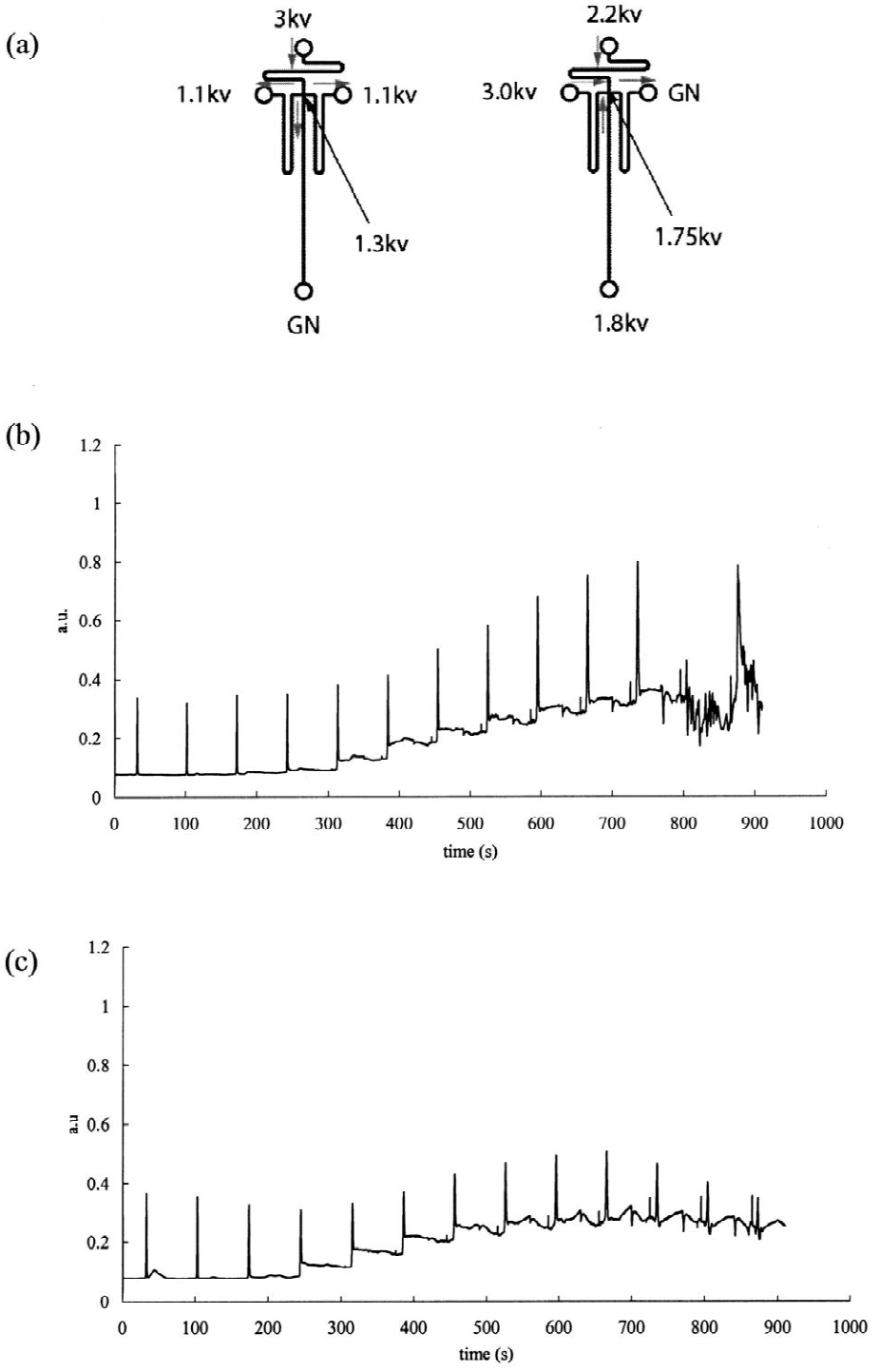


Fig. 6. The new chips were designed to reduce the back flow pressure effect by increasing the channel resistance. (a) Schematic design of the PDMS CE microchip with equal channel lengths and applied voltage at each reservoir. All channel lengths from the cross channel are 24 mm. Generally, as the channel length increased, pressure-driven back flows reduced. (b) and (c) Experimental results on the microchip with equal length. Different buffer volumes of 13 μl (b) and 10 μl (c) were used. As the buffer volume increased, the results became stable.

to (c), the volumes of buffer were larger, serial plug formations were more stable and pressure-driven back flow was reduced. When the volume of buffer is relatively of small quantity, only a slight change of the volume may have a great influence on sample separation. This is similar to the fact that the larger volume is less affected from the aspect of the change ratio. The calculation of the volume change ratio is shown in Table 3. If the channel lengths from the cross channel to SW are 3.5 and 24 mm, respectively, at the short and long channels, electric field strengths are 2500 and 729 V/cm, considering the applied voltage. In the calculation of increased buffer volumes, we only considered the injection mode in the two steps because the separation mode is trivial in terms of net flow compared to the injection mode. Electroosmotic mobility has already been calculated, and flow velocity, $V$, can also be obtained. Channel cross-sectional area $A$ is $2.5\times10^{-5}$ cm$^2$ and flow-rate, $Q$, is:

$$Q = VA \tag{3}$$

Assuming 10 serial injections were performed, the injection mode lasted 20 s each, and so the buffer volume can be obtained by multiplying flow-rate, $Q$, by the duration of the injection mode. Considering the inner diameter of the glass tip and PDMS reservoir size, we can calculate the increase in height of the reservoir and the buffer volume change ratio during the 10-serial injection mode. The buffer volume change ratios are 60, 11, 14.1, 18.3%, respectively, which match well with the real electopherogram obtained by serial injection. As the volume change ratio becomes smaller, the peak anomalies reduce less.

## 4. Conclusions

This paper presents the optimum design conditions for reducing the pressure effects on the CE microchip. Both hydrostatic flow and Laplace pressure at each reservoir generate a pressure-driven backflow reversing the direction of the EOF. The effects of the hydrostatic flow and Laplace pressure must be minimized to obtain a high throughput on the CE microchip and to carry out serial injection of sample. The changes in the level of buffer in each reservoir are inevitable. Based on the experiments, the following conclusions are given:

1. The hydrophilic property of the reservoirs is better than the hydrophobic one.
2. A longer channel from the cross channel to SW is better than short a channel because of channel resistance.
3. Larger buffer volumes reduce the influence of volume change ratio and thus minimize the anomalies.

We believe that these findings will be helpful in designing the multi-channel and serial injection mode chip in the future.

Table 3
Comparative data on three chip types: PDMS CE microchip without glass tip and with glass tip, and length equivalent CE microchip

| | Short length (13 μl) | Glass tip (70 μl) | Long waste length (13 μl) | Long waste length (10 μl) |
|---|---|---|---|---|
| Channel length (mm) | 3.5 | 3.5 | 24 | 24 |
| Electric field, $E$ (V/cm) | 2500 | 2500 | 729 | 729 |
| Flow-rate, $Q$ (cm$^3$/s) | $7.74\cdot10^{-5}$ | $7.74\cdot10^{-5}$ | $9.025\cdot10^{-6}$ | $9.025\cdot10^{-6}$ |
| Volume for $t=20$ s (cm$^3$) | $1.55\cdot10^{-3}$ | $1.55\cdot10^{-3}$ | $1.81\cdot10^{-4}$ | $1.81\cdot10^{-4}$ |
| Reservoir cross area (cm$^2$): $\pi/4\cdot(0.3)^2$ | $7.065\cdot10^{-2}$ | $7.065\cdot10^{-2}$ | $7.065\cdot10^{-2}$ | $7.065\cdot10^{-2}$ |
| Increased height (mm) | 0.11 | 0.11 | 0.026 | 0.026 |
| Sample volume (→equivalent value converted into height in reservoir) | 13 μl = $1.3\cdot10^{-2}$ cm$^3$ →1.84 mm | 70 μl = $7.0\cdot10^{-2}$ cm$^3$ →10 mm | 13 μl = $1.3\cdot10^{-2}$ cm$^3$ →1.84 mm | 10 μl = $1.0\cdot10^{-2}$ cm$^3$ →1.42 mm |
| Change volume (%) | 60 | 11 | 14.1 | 18.3 |

Calculated parts of channel length and applied voltage are from the cross channel to sample waste reservoir (SW).

## Acknowledgements

The authors appreciate Kee Chun Shin at Digital Bio Technology. This work has been supported by the Intelligent Microsystem Program (IMP) of the 21st Century Frontier R&D Program sponsored by the Korea Ministry of Science and Technology and also by the Nano Bioelectronics and Systems Research Center of Seoul National University, which is an Engineering Research Center supported by the Korean Science and Engineering Foundation (KOSEF).

## Appendix A

Hydrostatic flow (linear flow-rate) due to height difference in microchannel, $v_p$ (m/s), is given by:

$$v_p = \Delta h \rho g a^2 / 8\eta L \quad \text{(A.1)}$$

where $\Delta h$ is the height difference among the buffer reservoirs, $\rho$ is the buffer density, $g$ is the gravitational acceleration, $a$ is the capillary radius, $L$ is the channel length and $\eta$ is the buffer viscosity. In the etched capillaries, $D$ shapes, the Eq. (A.1) becomes:

$$v_p = \Delta h \rho g D_h^2 / (2 \cdot 15.626) \eta L \quad \text{(A.2)}$$

where $D_h$ is hydraulic diameter [$D_h = 4$(channel area/channel perimeter)]. Namely, if other parameters are kept constant during experiments, $v_p$ will be proportional to $\Delta h$. Thus, the EOF pumping produces different levels of the buffer in the each reservoir, $\Delta h$. Therefore, as $\Delta h$ increases the hydrostatic flow $v_p$ will affect the plug formation and produce the anomalies.

Laplace pressures are generated at meniscus interfaces and depend on the shape of the menisci. For a spherical meniscus surface, Laplace pressure, $\Delta P_L$ is:

$$\Delta P_L = 2\gamma / r \quad \text{(A.3)}$$

where $\gamma$ is the surface tension at the liquid–air interface (force/distance) and $r$ is the radius of curvature of the meniscus, defined by:

$$r = r_{reservoir} / \cos\theta \quad \text{(A.4)}$$

where $r_{reservoir}$ is the reservoir radius and $\theta$ is the contact angle.

## References

[1] A. Manz, D.J. Harrison, E.M.T. Verpoorte, J.C. Fettinger, A. Paulus, H. Lüdi, H.M. Widmer, J. Chromatogr. 593 (1992) 253.
[2] K. Seiler, D.J. Harrison, A. Manz, Anal. Chem. 65 (1993) 1481.
[3] D.F. Harrasion, K. Fluri, K. Seiler, Z. Fan, C.S. Effenhauser, A. Manz, Science 26 (1993) 895.
[4] S.C. Jacobson, R. Hergenröder, L.B. Koutny, J.M. Ramsey, Anal. Chem. 66 (1994) 1114.
[5] K.D. Altria, J. Chromatogr. A 856 (1999) 443.
[6] I. Medintz, W.W. Wong, G. Sensabaugh, R.A. Mathies, Electrophoresis 21 (2000) 2352.
[7] W. Xu, K. Uchiyama, T. Shimosaka, T. Hobo, J. Chromatogr. A 907 (2001) 279.
[8] C.L. Colyer, S.D. Mangru, D.J. Harrison, J. Chromatogr. A 781 (1997) 271.
[9] I. Rodriguez, Y. Zhang, H.K. Lee, S.F.Y. Li, J. Chromatogr. A 781 (1997) 287.
[10] J. Wang, A. Escarpa, M. Pumera, J. Feldman, J. Chromatogr. A 952 (2002) 249.
[11] Z.Q. Xu, T. Hirokawa, T. Nishine, A. Arai, J. Chromatogr. A 990 (2003) 53.
[12] D.R. Baker, in: Capillary Electrophoresis, Wiley-Interscience, New York, 1995, p. 98.
[13] H.J. Crabtree, E.C.S. Cheong, D.A. Tilroe, C.J. Backhouse, Anal. Chem. 73 (2001) 4079.
[14] G. Boer, A. Dodge, K. Fluri, B.H. van der Schoot, E. Verpoorte, N.F. de Rooij, in: D.J. Harrison, A.V. Den Berg (Eds.), Proceedings of the μTAS'98, Kluwer Academic, Dordrecht, 1998, p. 53.
[15] J.C. McDonald, D.C. Duffy, J.R. Anderson, D.T. Chiu, H. Wu, O.J.A. Schueller, G.M. Whitesides, Electrophoresis 21 (2000) 27.
[16] B.E. Slentz, N.A. Penner, E. Lugowska, F. Regnier, Electrophoresis 22 (2001) 3736.
[17] R.F. Probstein, in: H. Brenner (Ed.), Physicochemical Hydrodynamics, Butterworth, Stonham, MA, 1989, p. 267.
[18] X. Huang, M.J. Gordon, R.N. Zare, Anal. Chem. 60 (1988) 1837.
[19] J.W. Hong, T. Fujii, M. Seki, T. Yamamoto, I. Endo, Electrophoresis 22 (2001) 328.
[20] E.B. Cumming, S.K. Griffiths, R.H. Nilson, P.H. Paul, Anal. Chem. 72 (2000) 2526.
[21] G. Ocvirk, M. Munroe, T. Tang, R. Oleschuk, K. Westra, D.J. Harrison, Electrophoresis 21 (2000) 107.